Design and optimization of nanooptical couplers based on photonic crystals involving dielectric rods of varying lengths

ŞİRİN YAZAR

ÖZGÜR SALİH ERGÜL

Design and optimization of nanooptical couplers based on photonic crystals involving dielectric rods of varying lengths

Şirin YAZAR*, **Özgür ERGÜL**
Department of Electrical and Electronics Engineering, Faculty of Engineering,
Middle East Technical University, Ankara, Turkey

Abstract: This study presents design and optimization of compact and efficient nanooptical couplers involving photonic crystals. Nanooptical couplers that have single and double input ports are designed to obtain efficient transmission of electromagnetic waves in desired directions. In addition, these nanooptical couplers are cascaded by adding one after another to realize electromagnetic transmission systems. In the design and optimization of all these nanooptical couplers, the multilevel fast multipole algorithm, which is an efficient full-wave solution method, is used to perform electromagnetic analyses and simulations. A heuristic optimization method based on genetic algorithms is employed to obtain effective designs that provide the highest efficiency values. Two types of optimization strategies are applied using nanorods with a fixed length and using nanorods with varying lengths. This way, photonic crystals consisting of irregular arrays of both identical and nonidentical dielectric elements are designed for the realization of nanooptical couplers. The designs and their numerical results show that it is possible to design and further improve efficient nanooptical couplers with simple and compact geometries based on the principles of photonic crystals. Using relatively simple geometries and a single material, the designed nanooptical couplers are more preferable than the available designs in the literature.

Key words: Photonic crystals, nanooptical couplers, genetic algorithms, multilevel fast multipole algorithm

1. Introduction

Transmission of an electromagnetic wave in an intended direction and with a desired pattern is essential for proper functioning of most electronic devices. Photonic crystals, which are periodic sequences of dielectric unit cells, have been used in a plethora of electromagnetic applications for many years [1]. They are particularly useful in coupling and switching applications as they can be used to control and direct electromagnetic waves as desired [2–7]. Since they usually have relatively simple geometries, photonic crystals are easy to design and fabricate. They are used at optical frequencies and their dimensions are comparable to the operating wavelengths [8]. In particular, their size varies from 100 nanometers to several micrometers, making them suitable for designing and building small and compact optical structures. There is also a wide range of available materials that are appropriate to fabricate photonic crystals [9]. With these favorable properties, photonic crystals are suitable to design small, compact, and easy-to-manufacture nanooptical structures.

In photonic crystals, electromagnetic waves are not able to propagate in frequency ranges called the forbidden gaps of photons [10]. For a given structure, an electromagnetic wave is not transmitted and is reflected back if it is in this particular frequency range. This behavior of photonic crystals can be explained by Wulff-Bragg's interference condition. The incoming wave that is incident on a photonic crystal is divided into

---

*Correspondence: sirin.yazar@metu.edu.tr

different components as a result of diffraction and scattering, and when these components are superposed, if they interfere destructively, the transmitted waves cancel [11]. Therefore, whether a wave continues to propagate through a photonic crystal or not depends on the direction and phase of the wave. As a result, photonic crystal structures, working almost like waveguides, provide control over electromagnetic waves. In addition, at optical frequencies, photonic crystals made of dielectric elements are preferred more than metallic waveguides [11], as metals become lossy at high frequencies.

Dielectric elements in a photonic crystal should be arranged periodically, while the periodicity should be comparable to half of the wavelength to obtain directive property of photonic crystals. If well adjusted, defects created in a photonic crystal structure can localize electromagnetic energy, leading to resonances. As a result, the periodicity and arrangement of dielectric elements can be used to control the propagation of electromagnetic waves in desired directions and to prevent propagation in undesirable directions.

Couplers are often used to direct electromagnetic power from input(s) to desired output(s) in nanooptical systems. As the electronic devices become increasingly smaller, it becomes necessary to design smaller and more compact optical couplers. Moreover, achieving high levels of efficiency in the transmission of input power to desired output ports is another goal in the design of optical couplers. In fact, with the application of computational methods and optimization techniques, designing both efficient and small nanooptical couplers is possible [12]. In this study, we present compact and efficient nanooptical coupler designs based on photonic crystals consisting of dielectric nanorods to achieve electromagnetic transmission in different directions for either single or double inputs. The arrangements and lengths of dielectric rods are designed to efficiently transmit electromagnetic power to desired output ports while preventing transmission to undesired output regions. Applying on/off optimization and length optimization onto dielectric rods, the most efficient nanooptical coupler designs are obtained. Particularly, forward-transmitting couplers and 90-degree rotating couplers with single input and single output, as well as nanooptical couplers with double inputs are designed. Furthermore, adding these optical couplers one after another, cascaded designs are obtained to create different transmission systems. The numerical results demonstrate both the feasibility of efficient and compact nanooptical couplers based on photonic crystals, as well as the effectiveness of the developed optimization procedures.

2. Details of simulations and optimization trials

Some details of the numerical solver, optimization procedure, properties of nanorods, simulation parameters, and electromagnetic excitation considered in this study are explained in the following subsections.

2.1. Numerical solver

In this study, for full-wave numerical solutions of nanooptical structures involving photonic crystals, a fast and accurate solution method is employed. Method of moments (MoM), which is a well-known numerical solution method, is suitable for relatively simple electromagnetic problems, but for more complex problems involving higher computational loads, MoM is not convenient to use. Instead of solving matrix equations directly, they can be analyzed iteratively, resulting in $O(N^2)$ complexity per matrix-vector multiplication (MVM) for a problem with N unknowns. Unfortunately, for problems containing many numbers of unknowns, this complexity leads to long solution times and high memory usage. One of the methods used to reduce solution time and memory load is the fast multipole method (FMM), which makes the complexity per MVM $O(N^{3/2})$. The complexity is further reduced with multilevel fast multipole algorithm (MLFMA), where FMM is used in a recursive manner. In MLFMA, the three-dimensional Green's function is factorized by the Gegenbauer's addition theorem, and it

is diagonalized via plane waves at multiple levels such that the complexity per MVM is reduced to $O(N \log N)$. Hence, with the use of MLFMA, complex problems involving large numbers of unknowns can be solved efficiently with less computational load in comparison to other methods [13]. In the implementation of MLFMA, a tree structure is created by dividing the computational box that includes the object into subboxes subsequently at different levels. Only boxes that contain a part of the object are taken into account, while the other boxes are eliminated. The number of boxes at the lowest level is proportional to the number of unknowns. Subsequently, the electromagnetic interactions are performed in a group-by-group manner after they are categorized as near-field, far-field, and very far-field based on a one-box buffer scheme. This way, an MVM for an impedance matrix $\bar{\boldsymbol{Z}}$ can be decomposed into two parts as

$$\sum_{n=1}^{N} \bar{\boldsymbol{Z}}[m,n]\boldsymbol{a}[n] = \sum_{n=1}^{N} \bar{\boldsymbol{Z}}^{\mathrm{NF}}[m,n]\boldsymbol{a}[n] + \sum_{n=1}^{N} \bar{\boldsymbol{Z}}^{\mathrm{FF}}[m,n]\boldsymbol{a}[n] \quad (m = 1, 2, \ldots, N). \tag{1}$$

where $\bar{\boldsymbol{Z}}^{\mathrm{NF}}$ and $\bar{\boldsymbol{Z}}^{\mathrm{FF}}$ represent matrices involving near-field and far-field interactions, respectively. While near-field interactions are calculated directly and kept in memory, far-field interactions are computed on the fly at each iteration and are not kept in memory. These interactions are computed with the steps of aggregation, translation, and disaggregation. The radiated fields are calculated from the lowest level to the highest level of the tree structure in the aggregation step. At the lowest level, radiation patterns of the basis functions are shifted to the centers of the boxes, while at the higher levels, radiated fields are shifted between box centers based on child-parent relationships. Next, radiated fields are converted into incoming fields between far-zone boxes at the same levels in the translation step. In the third step, namely the disaggregation stage, incoming fields are calculated from the highest level to the lowest level. At the lowest level, incoming fields are received by the testing functions so that the MVM is completed.

2.2. Optimization procedure

In the design of nanooptical couplers, multiple parameters affect the efficiency of the designs. Hence, in a typical design procedure, a fast and efficient method is needed to realize large numbers of electromagnetic simulations to examine the effects of these parameters. Therefore, in this study, a GA-based optimization algorithm is integrated with MLFMA to obtain accurate solutions in a relatively short time [14]. The reason for which GA optimization is preferred is that GAs enable adjustable fitness functions and can lead to successful results even for large optimization spaces [15, 16].

In a GA optimization, firstly, a fitness function is defined such that the goal of the optimization is to minimize/maximize the value of this function. Therefore, how the fitness function is defined is one of the most important steps of optimization. A termination criterion should also be defined to complete an optimization, which can be either the total number of generations or a certain threshold for the value of fitness function such that the optimization can be stopped once the threshold is reached. In this study, the maximum number of generations is fixed as the termination criterion. In the first generation of an optimization, a random pool of 40 individuals, each of which has a chromosome that represents a possible solution, is created. Parameters of the optimization are encoded in terms of bits into chromosomes. The design corresponding to each individual at any generation is evaluated by the electromagnetic solver (MLFMA). Once all evaluations are completed for a generation, all individuals are sorted according to their fitness values, and the two best individuals are transferred to the next generation via elitism. Thus, during an optimization, the maximum value of the fitness function never deteriorates, remaining the same in two subsequent generations in the worst case. Following the

elitism of two individuals, the remaining 38 individuals of the next generation are determined by applying GA operations, such as mutation and crossover on parent chromosomes (tournament selection is used). According to the mutation rates determined at the beginning, the bits of the chromosomes are randomly inverted. Thus, it is aimed to increase the variety of the population and obtain chromosomes that potentially change the value of the fitness function in the desired direction. In crossover operations, new individuals are obtained from their parents by crossing over their chromosomes. This cycle continues until the last generation, and the best chromosome, i.e. the most successful individual, that provides the best fitness value is considered the output of the optimization, i.e. the optimal design. For example, in a typical on/off optimization, using binary encoding, 1 (on) can be used for the presence of a rod, while 0 (off) represents the absence of the associated rod.

In this study, two different kinds of optimizations are designed and performed: on/off optimization and length optimization. In both of these, the principle of operation is the same, but the variables are different. In an on/off optimization, dielectric rods are used as basic unit cells, and by making these rods present (on) or absent (off), we aim to reach optimal designs. For the designs considered in this study, a 10×10 array of dielectric rods is initially built, and 10×10 matrix is created for each 10×10 rod array in a way that each matrix element (either 0 or 1, which further corresponds to a bit in the associated chromosome) represents one rod in the array. Specifically, in such a matrix, which corresponds to an individual, the presence/absence of each rod in the array is represented by 1/0. On the other hand, in a length optimization, rods of 4 different lengths are used. As in on/off optimization, each rod is still represented by a number, but the rods of length 1500 nm, 2000 nm, 2500 nm, and 3000 nm correspond to 1, 2, 3, and 4, respectively, while 0 means that there is no rod. This way, each 10×10 matrix that consists of numbers 0, 1, 2, 3, and 4 represents an individual. By following the conventional steps of GA optimization, the most optimal design is obtained as a structure involving rods of different lengths. For an array of 100 nanorods of the same length, the number of possible configurations is $2^{100} \approx 1.27 \times 10^{30}$, while this number becomes even bigger when the nanorods are of different lengths. Fortunately, when GA-based optimization is applied, the number of solutions decreases to only $50 \times 40 = 2000$ for an optimization with 50 generations and 40 individuals at each generation.

For on/off optimizations, the total number of generations is determined as 50, while for length optimizations it is increased to 100 as the number of possible rod combinations is higher for the latter one. In both of these two kinds of optimizations, the symmetry in the arrangement of dielectric nanorods is not enforced.

2.3. Properties of nanorods

At the beginning of the design process of nanooptical couplers, a photonic crystal structure is formed by placing dielectric nanorods with square cross-sections in a 10×10 array. The center-to-center distance between adjacent rods is 300 nm, two times the edge length of each rod. Desired and undesired output regions are defined at the edges of these 10×10 arrays of nanorods. The nanorods are made of Si_3N_4 which has a relative permittivity of approximately 4 at 200 THz [17]. Si_3N_4 is an excellent choice for efficient nanooptical structures due to its fairly light weight, as well as its flexibility owing to its good flexural strength (850 mPa) that makes it favorable in fabrication processes [18]. The length of dielectric nanorods is kept at 2850 nm for on/off optimization, while for length optimization rods with 4 different lengths (1500 nm, 2000 nm, 2500 nm, and 3000 nm) are used.

2.4. Simulation parameters

In this study, the surface formulation used in the numerical solutions of nanooptical couplers is electric-magnetic current combined-field integral equation (JMCFIE). JMCFIE is a well-conditioned mixed formulation and it

gives accurate results especially for ordinary dielectric objects. Moreover, using it for low-contrast media with positive permittivity and permeability values usually leads to fewer numbers of iterations than other well-known formulations such as Poggio-Miller-Chang-Harrington-Wu-Tsai (PMCHWT) formulation and combined T formulation (CTF) [19–21]. Considering the relative permittivity of nanorods in this study, JMCFIE is a good choice for accurate and fast numerical analyses of photonic crystals. Rao-Wilton-Glisson (RWG) functions on triangular domains are used by using small triangles with respect to the wavelength [22] for discretization. The geometries to be optimized are discretized with a mesh size of $\lambda/10$ to keep the computational load low, while the final results of optimized nanooptical couplers presented in this study are obtained when the optimized geometries are discretized with a mesh size of $\lambda/20$ to increase accuracy. The frequency of operation is selected as 200 THz, which means the mesh size is chosen as 75 nm. The solution of each electromagnetic problem is obtained iteratively, and the generalized minimal residual (GMRES) method is used as the iterative solver.

2.5. Electromagnetic excitation

In this study, as the electromagnetic source of simulations, complex source point beam (CSPB) excitations are preferred since they have similar features as laser sources in nanooptical systems. CSPB, which can be made highly focused by controlling its parameters is used to provide highly intense electromagnetic power at the desired output ports. Particularly, when nanooptical couplers are cascaded by adding one after another, the path that electromagnetic waves have to propagate through becomes longer, which makes it better to use a focused excitation source, such as CSPB, that will enable high power transmission. Realization of CSPB is done by placing a Hertzian dipole in a location with complex coordinates, and the created incident fields due to CSPB can be written as

$$\bar{H}^{\mathrm{inc}}(\bar{r}) = \bar{I}_D \times \hat{R}\frac{\exp(ikR)}{4\pi R}\left(\frac{1}{R} - ik\right),\tag{2}$$

$$\bar{E}^{\mathrm{inc}}(\bar{r}) = i\omega\mu\frac{\exp(ikR)}{4\pi R}\left\{\bar{I}_D\left(1 + \frac{i}{kR} - \frac{1}{k^2R^2}\right) - \bar{I}_D\cdot\hat{R}\hat{R}\left(1 + \frac{3i}{kR} - \frac{3}{k^2R^2}\right)\right\}\tag{3}$$

with a dipole moment $\bar{I}_D$ located at $\bar{r}_D = \bar{r}_{D,R} + i\bar{r}_{D,I}$, where $\bar{R} = \bar{r} - \bar{r}_D = \hat{R}R$. The real part of the location, $\bar{r}_{D,R}$, specifies the real coordinates of the position of the beam, while the imaginary part, $\bar{r}_{D,I}$ specifies both the width and the direction of the beam. The magnitude of the imaginary part determines the width of the beam, while its sign indicates the propagation direction. Specifically, a positive sign corresponds to propagation in the negative direction along the corresponding path, whereas a negative sign means propagation in the positive direction.

3. Design, analysis, and optimization of nanooptical couplers

3.1. Defining fitness function

In the design of nanooptical couplers, our main goal is to maximize the electric field intensity at the desired output port while minimizing it at the other undesired output regions. Hence, the determination of a fitness function that will ensure the intended transmission condition is one of the most important parts of optimization with GA. Thus, the first step in this study is finding a proper fitness function that will result in the best designs of nanooptical couplers. A 10×10 array of dielectric nanorods with 300 nm center-to-center distance between them is used as the photonic crystal structure. This array, which extends from $x = -1.425\,\mu$m and

$y = -1.425\,\mu$m to $x = 1.425\,\mu$m and y= $1.425\,\mu$m, is centered at the origin. The aim is to design a forward-transmitting optical coupler, so the desired output region, Output Port-1, is located at the right edge of the array from $y = -0.125\,\mu$m to $y = 0.125\,\mu$m at $x = 1.400\,\mu$m while undesired output regions are located at the top edge, bottom edge, and regions around the desired output port on the right edge, as shown in Figure 1.
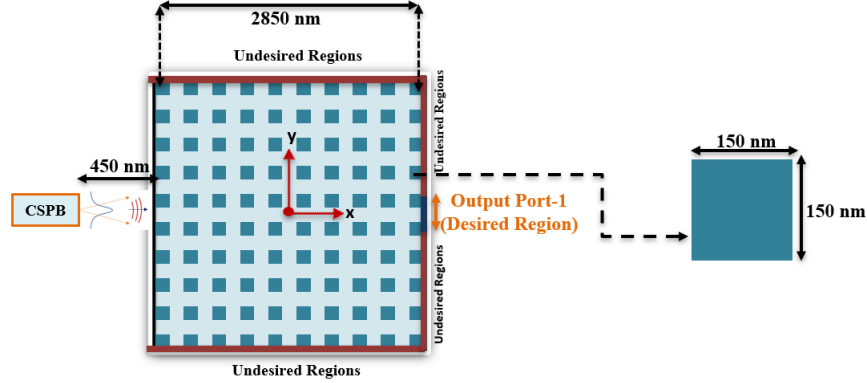

Figure 1. Desired and undesired transmission regions for a forward-transmitting coupler.

CSPB is used to excite the structure and placed 450 nm away from the structure at $x = (-1.875 - 5i)\,\mu$m, $y = 0\,\mu$m, $z = 0\,\mu$m in complex coordinates, while the incident wave from this source is polarized in the z direction.

Three different fitness functions, namely Fitness Function$_1$ (FF$_1$), Fitness Function$_2$ (FF$_2$), and Fitness Function$_3$ (FF$_3$), are defined as

$$\text{FF}_1 = \text{Max(Desired Fields)/Max(Undesired Fields)} \tag{4}$$

$$\text{FF}_2 = \text{Max(Desired Fields)} - \text{Max(Undesired Fields)} \tag{5}$$

$$\text{FF}_3 = \text{Max(Desired Fields)} - \text{Mean(Undesired Fields)} \tag{6}$$

and using these functions, the optimization trials are carried out with the simulation and optimization details given in Section 2. Here, in these equations, "Desired Fields" is the electric field intensity values (dBV/m) at the desired output region (Output Port-1) and "Undesired Fields" is the electric field intensity values (dBV/m) at the undesired output regions.

Table 1 shows mean electric field intensity values at Output Port-1 and at undesired output regions at the end of the optimization trials for a forward-transmitting coupler for these three fitness functions. Looking at this table, the third fitness function, FF$_3$ in Equation 6, is seen to provide the highest mean electric field intensity at Output Port-1 (34.4 dBV/m) while resulting in the lowest mean electric field intensity at undesired output regions (20.0 dBV/m). The highest difference between the mean electric field intensity at the desired port and undesired regions is 14.4 dB which is obtained with again FF$_3$. Hence, FF$_3$ is selected for the design of all nanooptical couplers presented in this study.

3.2. Forward-transmitting nanooptical coupler

In the design of a forward-transmitting optical coupler, the electromagnetic power transmission in the forward direction is maximized by increasing mean electric field intensity at Output Port-1 and decreasing it at the undesired output regions in Figure 1. The value of the fitness function with respect to generations and the resulting optimized rod array configuration are given in Figure 2.

Table 1. Mean electric field intensity values obtained via optimization trials using different fitness functions.

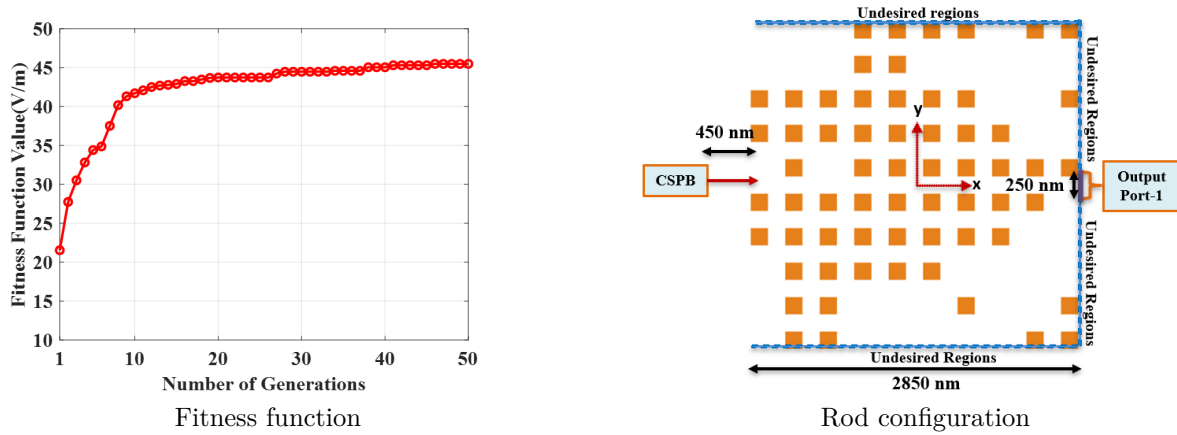| Fitness function	Mean/maximum E-field intensity at Output Port-1 (dBV/m)	Mean E-field intensity at undesired regions (dBV/m)
FF_1	28.9/29.6	21.1
FF_2	32.9/33.1	21.2
FF_3	34.4/35.8	20.0

Fitness function

Rod configuration

Figure 2. Fitness function and the resulting (optimized) rod configuration for a forward-transmitting coupler.

When the forward transmitting optical coupler is compared with the cases where there is no optical coupler (CSPB alone) and where there is a full array of dielectric rods (without any design process), the effectiveness of this design can be understood better. Near-zone electric field intensity distributions obtained when there is no nanooptical coupler or any other structure, i.e. CSPB alone, when there is a full 10×10 array of dielectric rods, and when there is the forward-transmitting optical coupler are given in Figure 3. Here, the near-zone electric field intensity distributions are numerically calculated in the x-y plane ($z = 0$) from $x = -2.2\,\mu$m and $y = -2.2\,\mu$m to $x = 2.2\,\mu$m and $y = 2.2\,\mu$m.

No coupler

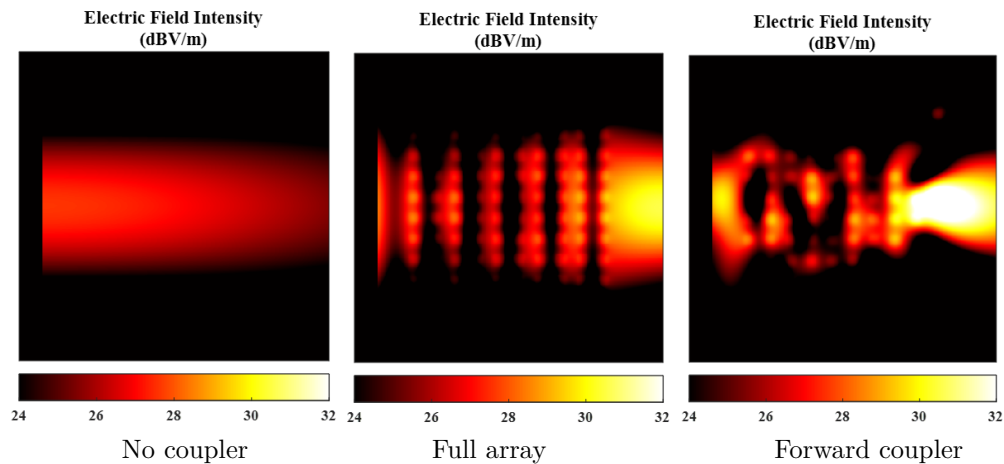Full array

Forward coupler

Figure 3. Near-zone electric field intensity when there is no coupler (left), when there is a full array of dielectric rods (middle), and when there is an optimized forward-transmitting nanooptical coupler (right).

Table 2 compares the designed nanooptical coupler with the cases when there is no structure (coupler) and when the full array of dielectric rods is used. According to the results in Table 2, the mean electric field intensity at the desired output port when the nanooptical coupler exists is 34.4 dBV/m which is 5.25 times the mean electric field intensity value at the undesired output regions (20.0 dBV/m). When there is the forward-transmitting nanooptical coupler, the mean electric field intensity at Output Port-1 is 2.6 times of the mean electric field intensity (at the same port) when there is no coupler and almost 1.9 times of the mean electric field intensity (at the same port) when the full array is used. Furthermore, the mean electric field intensity value at the undesired output regions is the lowest when the optimized nanooptical coupler exists. Considering these results, it is clear that the forward-transmitting nanooptical coupler optimized with FF_3 works successfully and effectively.

Table 2. Electric field intensity values when forward-transmitting coupler is used, in comparison to no-coupler and full-array cases.

Case	Mean/maximum E-field intensity at Output Port-1 (dBV/m)	Mean E-field intensity at undesired regions (dBV/m)
Forward-transmitting coupler	34.4/35.8	20.0
No coupler	26.1/26.2	22.3
Full array of rods	28.9/29.4	22.0

3.3. 90-degree nanooptical coupler

In the previous section, an optical coupler design for electromagnetic wave transmission in forward direction was presented. However, transmission through sharp bends and corners is also needed in various transmission problems which can be solved by designing nanooptical couplers [7, 23]. Therefore, in this study, we design an efficient and compact 90-degree nanooptical coupler applying on/off optimization with FF_3.

In Figures 4a and 4b, the values of the fitness function with respect to generations and the optimized rod array configuration are presented, respectively. In the optimization, the incident electromagnetic wave to Output Port-2 (desired output port) is maximized while the electric field intensity at the undesired regions is minimized. Here, Output Port-2 is located at the top edge of the array from $x = -0.125\,\mu\mathrm{m}$ to $x = 0.125\,\mu\mathrm{m}$ at $y = 1.400\,\mu\mathrm{m}$, as shown in Figure 4b. The near-zone electric field intensity distribution of the optimized 90-degree nanooptical coupler is given in Figure 4c. The maximum electric field intensity at Output Port-2 is 36.0 dBV/m for the optimized coupler. Besides, the mean electric field intensity value at Output Port-2 is 33.8 dBV/m, while the mean electric field intensity value at the other output regions is 22.2 dBV/m, corresponding to 11.6 dB difference between them. We conclude that the optimized 90-degree coupler can successfully couple incoming waves to Output Port-2, despite the challenging nature of the operation.

3.4. Double-input nanooptical couplers

Nanooptical couplers with double input ports are needed at junctions of a nanooptical transmission system, where we need to transmit the incoming electromagnetic waves from two input sources to the desired output port while preventing power transmission towards the undesirable output regions. Therefore, in this study, we design and examine three different double-input nanooptical coupler designs. For the first design, one CSPB is placed at $x = (-1.875 - 5i)\,\mu\mathrm{m}$, $y = 0\,\mu\mathrm{m}$, $z = 0\,\mu\mathrm{m}$ in the complex coordinates, while the other one is placed at $x = 0\,\mu\mathrm{m}$, $y = (-1.875 - 5i)\,\mu\mathrm{m}$, $z = 0\,\mu\mathrm{m}$. In both cases, the incident wave is polarized in the z direction.

Fitness function   Rod configuration   Electric field intensity
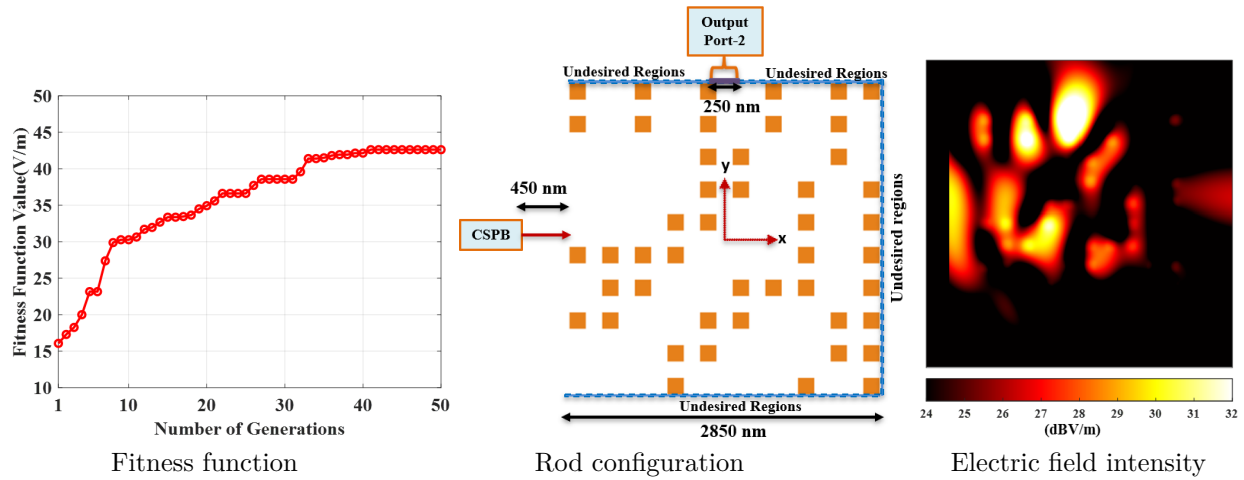
Figure 4. Fitness function, optimized rod configuration, and near-zone electric field intensity distribution for 90-degree nanooptical coupler.

The desired output port, Output Port-1, is located at the right edge of the array from $y = -0.125\,\mu$m to $y = 0.125\,\mu$m at $x = 1.400\,\mu$m. The goal of the optimization is to maximize the electric field intensity at Output Port-1 and minimize it at other undesired output regions. Figures 5a and 5b show the values of fitness function with respect to number of generations, and the rod configuration obtained at the end of the on/off optimization, respectively. Near-zone electric field intensity distribution of this nanooptical coupler design is given in Figure 5c. The mean electric field intensity at Output Port-1 is 36.8 dBV/m, while the mean electric field intensity at undesired output regions is 24.0 dBV/m, with a difference of 12.8 dB. Furthermore, the maximum electric field intensity at the desired output port becomes 37.8 dBV/m. Hence, with this design, electromagnetic transmission is effectively established towards Output Port-1.
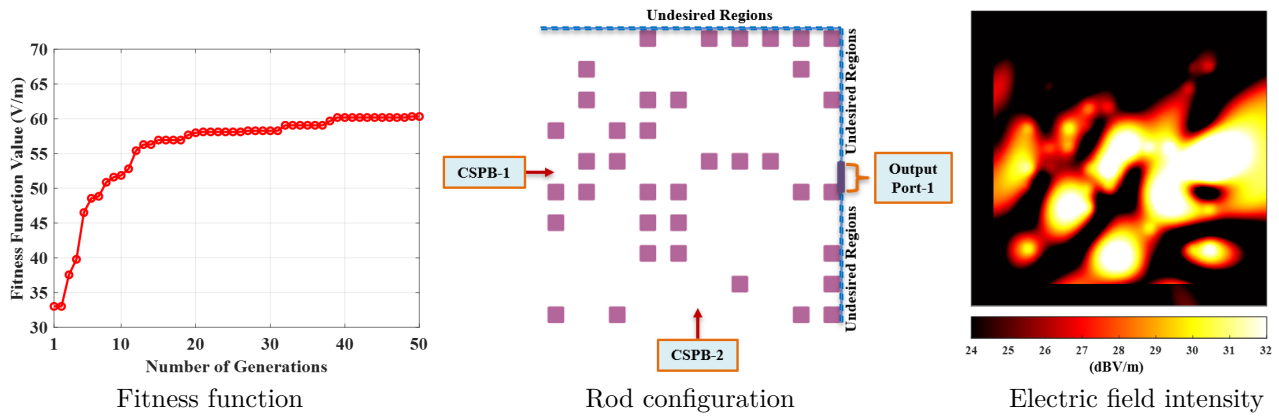

Fitness function   Rod configuration   Electric field intensity

Figure 5. Optimization results for the first design of double-input nanooptical coupler.

In the second and third designs, 10×20 dielectric rod arrays are used, unlike the first double-input nanooptical coupler using the standard 10×10 grid. The nanooptical couplers are centered at the origin and they cover a rectangular area extending from $x = -2.925\,\mu$m, $y = -1.425\,\mu$m to $x = 2.925\,\mu$m, $y = 1.425\,\mu$m in the x-y plane. In the second design, one CSPB source is positioned at $x = -1.425\,\mu$m, $y = -1.875 - 5i\,\mu$m, $z = 0\,\mu$m, while the other CSPB is positioned at $x = 1.425\,\mu$m, $y = -1.875 - 5i\,\mu$m, $z = 0\,\mu$m. Both

excitations generate z-polarized waves, which are intended to be combined and transmitted to Output Port-1 in Figure 6a. This port is positioned at the top edge of the rod array from $x = -1.625\,\mu$m to $x = -1.375\,\mu$m at $y = 1.400\,\mu$m. The resulting rod configuration and the near-zone electric field intensity plot for the second design are given in Figures 6a and 6b, respectively. In the third design, one CSPB source is positioned at $x = -3.375 - 5i\,\mu$m, $y = 0\,\mu$m, $z = 0\,\mu$m, while the other one is positioned at $x = 3.375 + 5i\,\mu$m, $y = 0\,\mu$m, $z = 0\,\mu$m. Similar to the previous case, z-polarized waves emerging from these sources are to be collected at Output Port-1 in Figure 6c, which is positioned as in the previous case. The optimized rod configuration and the near-zone electric field intensity plot for the third design are given in Figures 6c and 6d, respectively.

The difference between the mean electric field intensity at Output Port-1 (38.0 dBV/m) and mean electric field intensity at undesired output regions (24.0 dBV/m) for the second design is 14 dB. For the third design, the mean electric field intensity at Output Port-1 is 35.7 dBV/m, while the mean electric field intensity at undesired output regions is 25.6 dBV/m, leading to a difference of 10.1 dB. Consequently, we conclude that all three designs provide successful results in terms of optimization aims and they are functional by providing the desired results for given input and output locations.
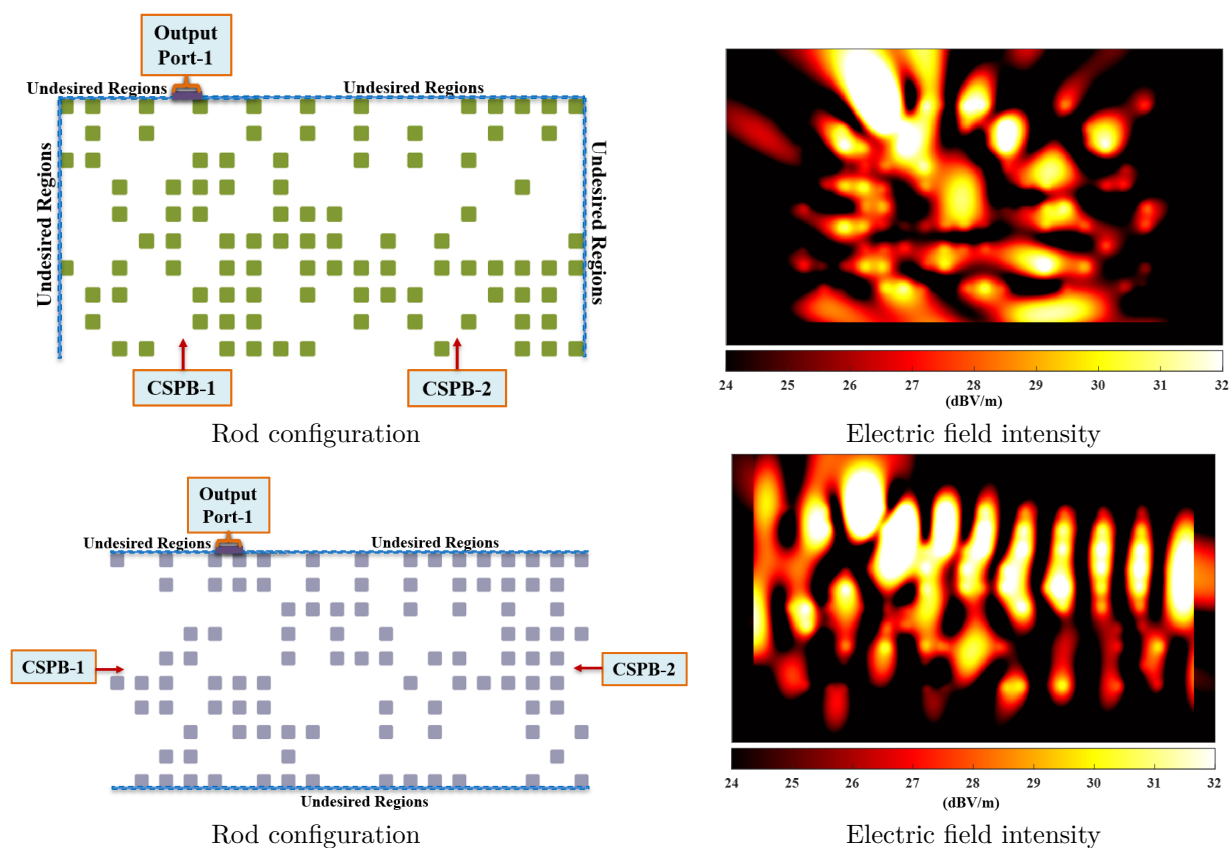

Rod configuration

Electric field intensity

Rod configuration

Electric field intensity

Figure 6. Optimization results for the second (a,b) and third (c,d) designs of double-input nanooptical couplers.

4. Cascaded nanooptical couplers

Cascaded nanooptical couplers, where it is aimed to construct transmission systems by combining the designed nanooptical couplers one after another, are also discussed as a part of this study. To demonstrate working

principles of cascaded couplers, we consider combinations involving two couplers. The first coupler is excited with CSPB, while the subsequent coupler uses the output of the first coupler as input to operate as it is designed. The near-zone electric field intensities are numerically calculated in the x-y plane ($z = 0$) from $x = -3.7\,\mu$m and $y = -2.2\,\mu$m to $x = 3.7\,\mu$m and y= $2.2\,\mu$m and their plots for CSPB alone (without any couplers) and for the cascaded couplers are given in Figure 7.

No coupler

Cascaded forward-transmitting couplers

Cascaded forward and 90-degree couplers

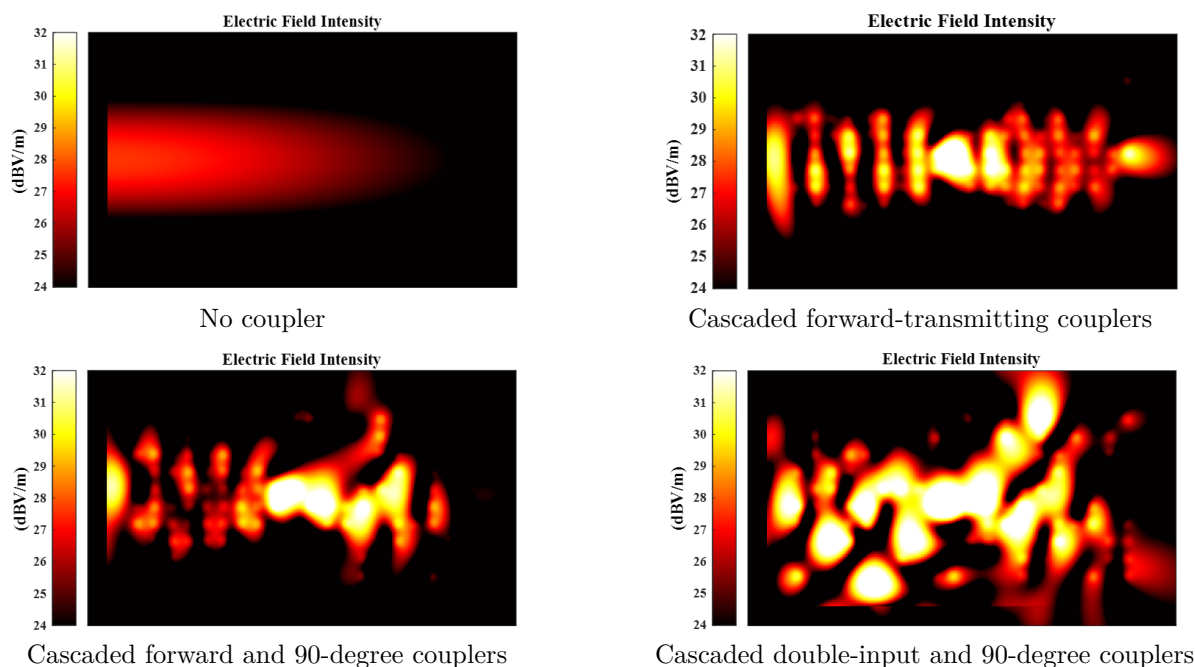Cascaded double-input and 90-degree couplers

Figure 7. Near-zone electric field intensity distributions without and with cascaded couplers.

Without nanooptical couplers, that is, only with CSPB, the mean electric field intensity value obtained at the locations of Output Port-1 is 23.7 dBV/m, given in Figure 7a, while the mean electric field intensity value when two forward-transmitting couplers are cascaded is increased to 30.1 dBV/m as given in Figure 7b. Similarly, when only CSPB exists, the mean electric field intensity value obtained at the locations of Output Port-2 is 21.2 dBV/m, which is increased to 26.5 dBV/m when a 90-degree nanooptical coupler is cascaded with a forward transmitting nanooptical coupler as shown in Figure 7c. Finally, when the cascaded system in Figure 7d, which is obtained by cascading a 90-degree nanooptical coupler with a double-input nanooptical coupler, is used, the mean electric field intensity value obtained at the locations of Output Port-2 increases to 32.8 dBV/m from 21.2 dBV/m. According to these results, we conclude that the designed nanooptical couplers can successfully be cascaded to transmit electromagnetic power to desired directions in a controlled manner. Remarkably, the couplers designed for CSPB excitations operate well when they are excited via another coupler, which makes the cascade operation possible by providing sufficient power to be transmitted to a desired location.

5. Design, analysis, and optimization of nanooptical couplers with length optimization

The electromagnetic excitation beams, such as a CSPB, have a 3D radiation, so not only the rod configurations but also the length of the rods may affect the transmission efficiency of nanooptical coupler designs. Hence, in this part of the study, the length of the rods is also made an optimization parameter to improve the transmission

performances of the nanooptical couplers which are designed with on/off optimization alone. The details of length optimization and descriptions on how it works are given in Section 2.2. The simulation parameters such as excitation, frequency, numerical solver are all the same as before while the only difference is using the rods with four different lengths which are 1500 nm (Rod-1), 2000 nm (Rod-2), 2500 nm (Rod-3), and 3000 nm (Rod-4). As previously explained, each rod length is represented by an integer, i.e. 1500 nm, 2000 nm, 2500 nm, and 3000 nm correspond to 1, 2, 3, and 4, respectively, while 0 corresponds to the absence of any rods. Therefore, a 10×10 matrix that consists of elements with values equal to either 0, 1, 2, 3, or 4 represents a possible design involving rods with different lengths. As in on/off optimization, the design that provides the highest fitness function value becomes the most efficient nanooptical coupler.

5.1. Forward-transmitting nanooptical coupler

Applying length optimization, an array of 10×10 dielectric rods with different lengths is obtained which successfully results in transmission of the electromagnetic wave from input to the desired output port, Output Port-1, while minimizing electric field intensity at undesired output regions. After 100 generations of length optimization, the matrix representation, rod configurations, and near-zone electric field intensity distribution for the forward-transmitting coupler are given in Figure 8.
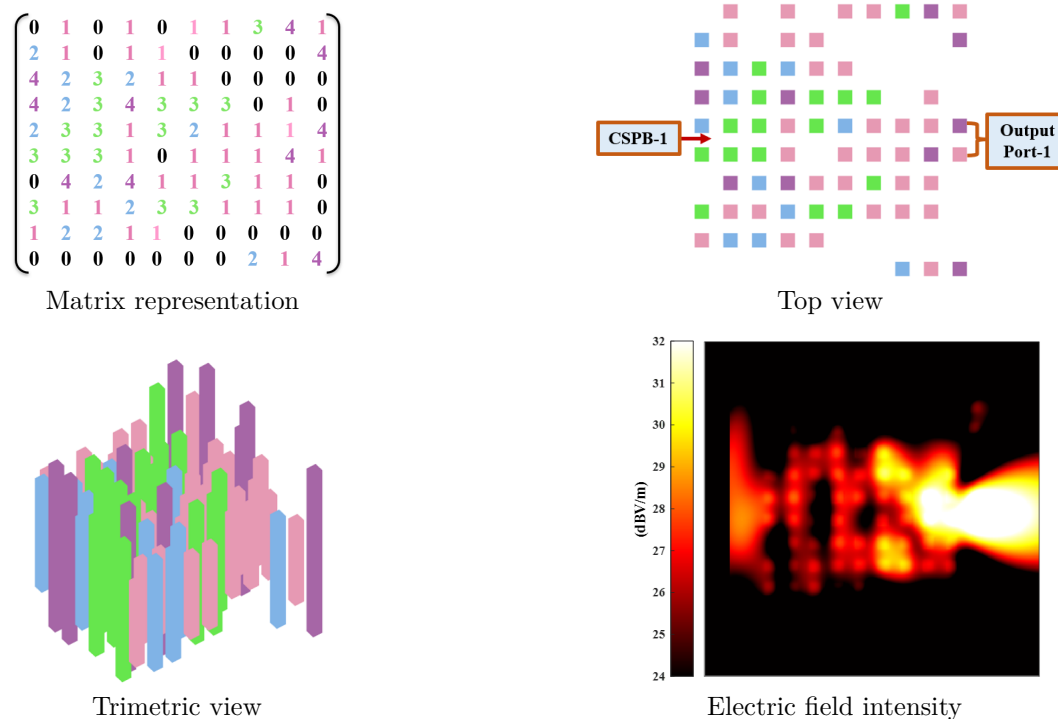

Matrix representation

Top view

Trimetric view

Electric field intensity

Figure 8. Optimization results for forward-transmitting coupler design obtained via length optimization.

In Table 3, the results of on/off optimization and length optimization are given for forward-transmitting nanooptical coupler. According to these results, the change in rod lengths definitely leads to improvement in the transmission. The maximum electric field intensity at the desired output port is increased to 36.4 dBV/m, while the mean electric field intensity at the same port reaches 35.7 dBV/m which means an increase by 16.1% compared to the previous design with on/off optimization. Moreover, the difference between the mean electric

field intensity values at Output Port-1 and undesired output regions is increased to 15.4 dBV/m. Hence, comparing the forward-transmitting couplers designed via length optimization and on/off optimization, it can be said that the length optimization provides a better design.

Table 3. Comparison of on/off optimization and length optimization to design forward-transmitting couplers.

Case	Mean/maximum E-field intensity at Output Port-1 (dBV/m)	Mean E-field intensity at undesired regions (dBV/m)
On/off optimization	34.4/35.8	20.0
Length optimization	35.7/36.4	20.3

5.2. 90-degree nanooptical coupler

The second design with length optimization is a 90-degree nanooptical coupler. This time the aim is to obtain an array of 10×10 dielectric rods with different lengths such that the structure directs the electromagnetic wave from the input CSPB source to Output Port-2. Figure 9 shows the optimized matrix representation, the corresponding rod configuration, and near-zone electric field intensity distribution for the optimal 90-degree nanooptical coupler design after 100 generations of length optimization. The numerical comparison of the designs obtained with on/off optimization and length optimization are given in Table 4. According to these results, via length optimization, the mean electric field intensity at Output Port-2 is increased to 34.4 dBV/m, while the mean electric field intensity in the undesired output regions is 22.7 dBV/m resulting in a difference of 11.7 dB. In addition, the maximum electric field intensity at Output Port-2 increases to 36.6 dBV/m. Thus, the change in rod lengths leads to the improvement in the design.
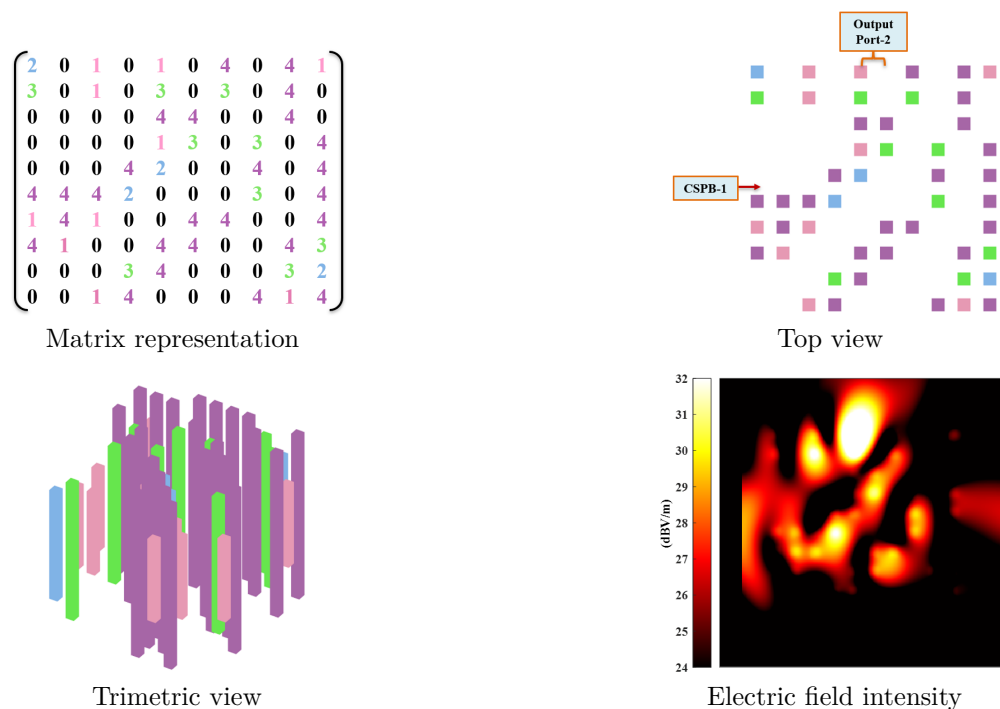

Matrix representation

Top view

Trimetric view

Electric field intensity

Figure 9. Optimization results for 90-degree coupler design obtained via length optimization.

Table 4. The comparison of on/off and length optimization trials to design 90-degree nanooptical couplers.

Case	Mean/maximum E-field intensity at Output Port-2 (dBV/m)	Mean E-field intensity at undesired regions (dBV/m)
On/off optimization	33.8/36.0	22.2
Length optimization	34.4/36.6	22.7

5.3. Double-input nanooptical coupler

The last design with length optimization is an improved double-input nanooptical coupler. Two CSPB sources are located as shown in 5b. The aim is to maximize the electric field intensity at Output Port-1 shown in the same figure. Figure 10 shows the optimized rod configuration, the corresponding matrix representation, and the near-zone electric field intensity distributions for the double-input nanooptical coupler designed by length optimization at the end of 100 generations. According to numerical results obtained, the mean electric field intensity in undesired output regions is 25.5 dBV/m, while the mean and the maximum electric field intensity at Output Port-1 is 38.7 dBV/m and 39.7 dBV/m, respectively. Comparing these results with the ones obtained by the previously designed double-input coupler via on/off optimization, it can be said that the length optimization improves the transmission efficiency and enhances the difference between the mean electric field intensity at Output Port-1 and the mean electric field intensity in undesired output regions.
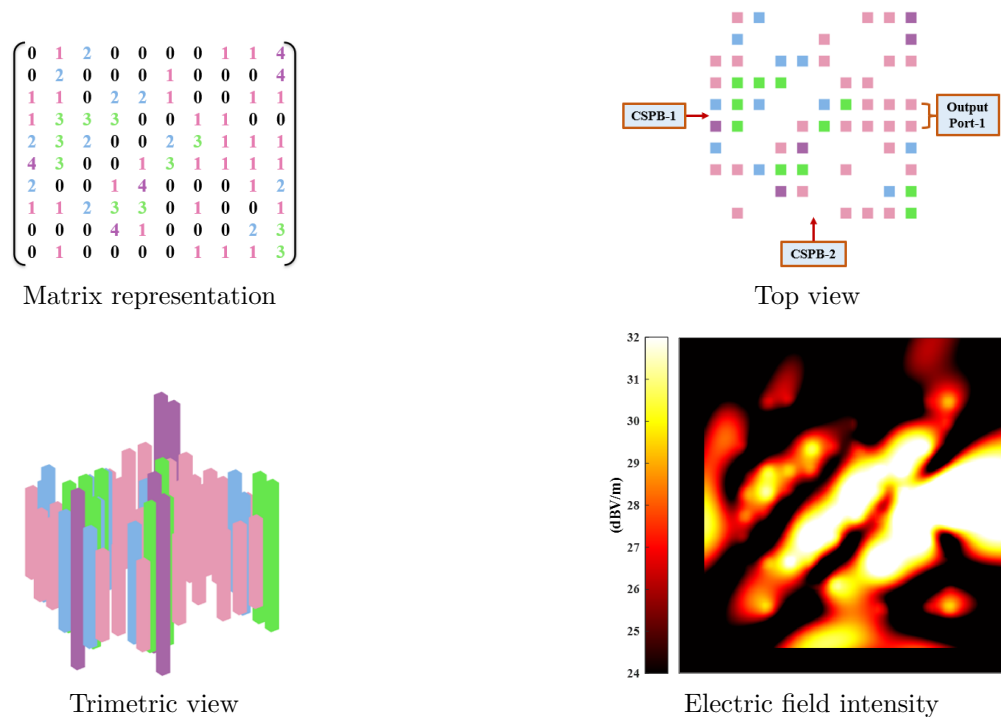

Matrix representation

Top view

Trimetric view

Electric field intensity

Figure 10. Optimization results for double-input coupler design obtained via length optimization.

6. Conclusion

In this study, various nanooptical couplers involving photonic crystals were designed and analyzed. Firstly, forward-transmitting and 90-degree nanooptical couplers were designed based on on/off optimization of dielectric nanorod arrangements. The effectiveness of the coupler designs that can be used both as repeaters (forward-transmitting) and in bent transmission lines was shown in detail. In addition to these single-input nanooptical couplers, double-input nanooptical couplers were designed to be used in electromagnetic wave transmission at junction locations. The numerical results proved that these designs effectively transmit waves in the desired directions. These coupler designs were also examined when one of them is added after another to create electromagnetic transmission systems. In order to improve the designs, not only on/off optimization trials but also length optimization trials were designated and performed. It is shown that an effective integration of GAs and MLFMA enables the efficient design of compact nanooptical couplers that can be used in a plethora of applications. Compact and efficient structures presented in this study make contributions to the rapidly developing technology, where nanooptical systems with smaller components are required to build more functional systems. Since the designed nanooptical couplers have relatively simple geometries and are based on only one material, they are favorable compared to many other couplers in the literature. The feasibility of various compact nanooptical couplers that possess novel characteristics, such as variable lengths can be considered a starting point for the future designs of more complicated nanooptical systems involving these couplers.

References

[1] Joannopoulos JD, Johnson SG, Winn JN, Meade RD. Photonic Crystals: Molding The Flow of Light. 2nd ed. Princeton, NJ, USA: Princeton University Press, 2008.

[2] Talneau A, Lalanne P, Agio M, Soukoulis CM. Low-reflection photonic-crystal taper for efficient coupling between guide sections of arbitrary widths. Optics Letters 2002; 27 (17): 1522–1524. doi: 10.1364/OL.27.001522

[3] Pissoort D, Michielssen E, Ginste DV, Olyslager F. Fast-multipole analysis of electromagnetic scattering by photonic crystal slabs. Journal of Lightwave Technology 2007; 25 (9): 2847–2863. doi: 10.1109/JLT.2007.902771

[4] Mekis A, Chen JC, Kurland I, Fan S, Villeneuve PR et al. High transmission through sharp bends in photonic crystal waveguides. Physical review letters 1996; 77 (18): 3787–3790. doi: 10.1103/PhysRevLett.77.3787

[5] Gagnon D, Dumont J, Dubé LJ. Beam shaping using genetically optimized two-dimensional photonic crystals. Journal of the Optical Society of America A 2012; 29 (12): 2673–2678. doi: 10.1364/JOSAA.29.002673

[6] Ergül Ö, Malas T, Gürel L. Analysis of dielectric photonic-crystal problems with MLFMA and Schur complement preconditioners. Journal of Lightwave Technology 2011; 29 (6): 888–897.

[7] Altınoklu A, Ergül Ö. Nano-optical couplers for efficient power transmission along sharply bended nanowires. Applied Computational Electromagnetics Society Journal 2019; 34 (2): 228–233.

[8] Skorobogatiy M, Yang J. Fundamentals of Photonic Crystal Guiding. Cambridge, England: Cambridge University Press, 2009.

[9] Lopez C. Materials aspects of photonic crystals. Advanced Materials 2003; 15 (20): 1679–1704. doi: 10.1002/adma.200300386

[10] Spielmann C, Szipöcs R, Stingl A, Krausz F. Tunneling of optical pulses through photonic band gaps. Physical Review Letters October 1994; 73 (17): 2308–2311. doi: 10.1103/PhysRevLett.73.2308

[11] Yablonovitch E. Photonic band-gap structures. Journal of the Optical Society of America B 1993; 10 (2): 283–295. doi: 10.1364/JOSAB.10.000283

[12] Karaosmanoğlu B, Yazar Ş, Ergül Ö. Design of compact nano-optical couplers involving dielectric nanorods. In: 2nd URSI Atlantic Radio Science Meeting (AT-RASC); Gran Canaria, Spain; 2018. pp. 1-3.

[13] Ergül Ö, Gürel L. The Multilevel Fast Multipole Algorithm (MLFMA) For Solving Large-Scale Computational Electromagnetics Problems. Hoboken, NJ, USA: Wiley, 2014.

[14] Önol C, Karaosmanoğlu B, Ergül Ö. Efficient and accurate electromagnetic optimizations based on approximate forms of the multilevel fast multipole algorithm. IEEE Antennas and Wireless Propagation Letters 2015; 15: 1113–1115. doi: 10.1109/LAWP.2015.2495237

[15] Rahmat-Samii Y, Michielssen E. Electromagnetic optimization by genetic algorithms. Microwave Journal 1999; 42 (11): 232–232.

[16] Johnson JM, Rahmat-Samii Y. Genetic algorithms in electromagnetics. In: IEEE Antennas and Propagation Society International Symposium; Baltimore, MD, USA; 1996. pp. 1480–1483.

[17] Luke K, Okawachi Y, Lamont MR, Gaeta AL, Lipson M. Broadband mid-infrared frequency comb generation in a Si3N4 microresonator. Optics Letters 2015; 40 (21): 4823–4826. doi: 10.1364/OL.40.004823

[18] Liu J, Zhu T, Xie ZP, Wu W. New route to improve the flexural strength of silicon nitride ceramics by introducing tungsten carbide nanoparticles. International Journal of Applied Ceramic Technology 2017; 14 (5): 860–865. doi: 10.1111/ijac.12732

[19] Ergül Ö, Gürel L. Comparison of integral-equation formulations for the fast and accurate solution of scattering problems involving dielectric objects with the multilevel fast multipole algorithm. IEEE Transactions on Antennas and Propagation 2009; 57 (1): 176–187. doi: 10.1109/TAP.2008.2009665

[20] Yla-Oijala P, Taskinen M. Application of combined field integral equation for electromagnetic scattering by dielectric and composite objects. IEEE Transactions on Antennas and Propagation 2005; 53 (3): 1168–1173. doi: 10.1109/TAP.2004.842640

[21] Karaosmanoğlu B, Ergül Ö. Modified combined tangential formulation for stable and accurate analysis of plasmonic structures. In: International Applied Computational Electromagnetics Society Symposium (ACES); Firenze, Italy; 2017. pp. 1-2.

[22] Rao S, Wilton D, Glisson A. Electromagnetic scattering by surfaces of arbitrary shape. IEEE Transactions on Antennas and Propagation 1982; 30 (3): 409–418. doi: 10.1109/TAP.1982.1142818

[23] Tunçyürek YE, Karaosmanoğlu B, Ergül Ö. Computational design of optical couplers for bended nanowire transmission lines. Applied Computational Electromagnetics Society Journal 2017; 32 (7): 562-568.